Vol. 45 — N° 3 09 21 p. 583–598

GEOSTANDARDS and GEOANALYTICAL RESEARCH

Boron Mass Fractions and $\delta^{11}B$ Values of Eighteen International Geological Reference Materials

Guanhong **Zhu** (1, 2), Jinlong **Ma** (1)*, Gangjian **Wei** (1) and Le **Zhang** (1)

(1) State Key Laboratory of Isotope Geochemistry, Guangzhou Institute of Geochemistry, Chinese Academy of Sciences, Guangzhou 510640, China
(2) University of Chinese Academy of Sciences, Beijing 100049, China
* Corresponding author. e-mail: jlma@gig.ac.cn

Here we report boron (B) mass fractions and $\delta^{11}B$ values of a set of geological reference materials including ultramafic rocks, basalts, andesites, felsic rocks and sedimentary materials. Boron was purified using a single column loaded with AGMP-1 resin. The $\delta^{11}B$ data were determined by multi-collector inductively coupled plasma-mass spectrometry (MC-ICP-MS) using the sample-standard bracketing method, and the NIST SRM 951 reference solution was selected as the calibrator. Boron mass fractions were measured by ICP-MS. Based on analyses of the NIST SRM 951 reference solution over a period of 1 year, the *intermediate measurement precision* for B isotope determinations was better than 0.5‰ (2*s*). The robustness of the overall B isotope analytical procedure was evaluated by carrying out replicate analyses of five reference materials (i.e., B5, JB-2, JB-3, B6 and JR-2). The eighteen geological reference materials have $\delta^{11}B$ values ranging from -28.85 to +10.47‰ and B mass fractions ranging from 2.37 to 158 µg g^{-1}. The comprehensive data set presented here serves as a reference for quality assurance and comparison of B isotope and B mass fraction data among different laboratories.

Keywords: boron, B isotope compositions, B mass fractions, MC-ICP-MS, geological reference materials.

Received 18 Aug 20 – Accepted 20 May 21

Boron (B) is a moderately volatile, lithophile and soluble element. It has two stable isotopes, ^{10}B and ^{11}B, with abundances of 19.9 and 80.1%, respectively (Rosman and Taylor 1988). Given its high geochemical reactivity (Xiao *et al.* 2013) and the large relative mass difference between ^{10}B and ^{11}B, boron isotopes have become a powerful tool to trace various geological processes, such as continental erosion (Rose *et al.* 2000, Lemarchand and Gaillardet 2006, Ercolani *et al.* 2019, Mao *et al.* 2019), the evolution of the crust-mantle system (Marschall *et al.* 2017), subduction-related processes (Tonarini *et al.* 2011, Scambelluri and Tonarini 2012, Li *et al.* 2016, 2019a), ancient marine environments (Yu *et al.* 2010, Rae *et al.* 2011, Rasbury and Hemming 2017, Raitzsch *et al.* 2018, Chen *et al.* 2019) and mineralisation and ore genesis (Garda *et al.* 2009, Pal *et al.* 2010, Lambert-Smith *et al.* 2016, Zhang *et al.* 2019). However, the analysis of boron isotopes in silicate materials has encountered difficulties such as potential contamination, vapour loss and poor recovery during digestion, chromatographic purification and concentration processes. These challenges have hindered the routine analysis of B isotope compositions in silicate rocks, resulting in limited database of the B isotope compositions of geological materials.

Generally, two methods, fusion and acid digestion, have been used to digest silicates for B content and isotope analysis (Liu *et al.* 2018). The fusion method is very effective in decomposing silicate rocks (Kiss 1988), but it has a high procedural blank for B (37–50 ng; Tonarini *et al.* 1997, Lemarchand *et al.* 2012). Acid digestion, in contrast, involves a lower B blank (1–20 ng), and it is thus the most widely used digestion method for B isotope analysis in silicate samples (Nakamura *et al.* 1992, Wei *et al.* 2013, Pi *et al.* 2014, Liu *et al.* 2018). However, in these acidic media (containing HF), boron readily forms BF_3, which is easy to volatilise (Nakamura *et al.* 1992). Therefore, the chemical extraction of boron from silicate samples encounters difficulties such as vapour loss and potential contamination during the long concentration process.

Silicate matrices contain a large number of elements (such as Si, Al and Ti) whose elutions on ion exchange resins

doi: 10.1111/ggr.12397

are similar to that of boron, which makes the separation of boron in rock more complicated. Therefore, in the original studies, the purification of boron from silicates involved at least three ion exchange columns (Nakamura *et al.* 1992, Tonarini *et al.* 1997). These procedures need to strictly control the potential contamination of the sample from prolonged sample processing and are time-consuming. More recently, Wei *et al.* (2013) developed a simple separation procedure using a single column loaded with AGMP-1 anion exchange resin to purify B from silicates. This technique greatly simplifies the purification process of B but requires a large quantity of potentially hazardous chemicals (24 mol l^{-1} HF). In addition, B can be purified by non-exchange resin methodologies. For example, Pi *et al.* (2014) presented a micro-sublimation technique for boron purification in silicates. This technique is simple and does not rely on ion exchange resin, but it requires ensuring that most silicon from the sample is removed during the dissolution process and is not suitable for the separation of samples with low B contents (< 5 μg g^{-1}).

Measurements of B mass fraction are generally carried out with prompt gamma activation analysis (PGAA), inductively coupled plasma-atomic emission spectrometry (ICP-AES) or ICP-MS (e.g., Gonfiantini *et al.* 2003, Gméling *et al.* 2005, Leeman *et al.* 2017). Boron isotope compositions are commonly measured by positive ion thermal ionisation mass spectrometry (P-TIMS), negative ion thermal ionisation mass spectrometry (N-TIMS) or MC-ICP-MS (Foster *et al.* 2018, Marschall and Foster 2018). The P-TIMS method, where $Cs_2BO_2^+$ (masses 308 and 309) are measured, involves the minimum instrumental mass fractionation and most of B isotope measurements for silicates were performed by this method (e.g., Nakamura *et al.* 1992, Tonarini *et al.* 1997, Rosner and Meixner 2004, Leeman *et al.* 2017). The N-TIMS approach can achieve accuracy and precision of ± 0.4–0.7‰ (at 95% confidence) on sample sizes as small as 1 ng of B (Foster *et al.* 2018). However, these two approaches are time-consuming. In comparison, MC-ICP-MS offers several distinct advantages including rapid sample analysis (~ 8 min) and the mass bias can be corrected by sample-standard bracketing (SSB) method and can achieve precision of < 0.5‰ (2*s*, e.g., Wei *et al.* 2013).

Although the analytical precision of B mass fraction and B isotope measurement has improved significantly in the past two decades, there is still considerable indeterminacy in the accurate measurement of B mass fractions and B isotope ratios in some geological materials. This issue can be demonstrated by the insufficient agreement of B mass fractions reported for some reference materials (i.e., JG-2, UB-N and PCC-1; Gladney *et al.* 1991, Govindaraju 1994, Harvey *et al.* 1996, D'Orazio 1999, Romer *et al.* 2014, Peters and Pettke 2017) and inconsistent $\delta^{11}B$ values for some reference materials measured by different laboratories, such as B1, B2, B4, B5, B6, B7 and AGV-2 (Gonfiantini *et al.* 2003, Pi *et al.* 2014, Liu *et al.* 2018). For example, Gonfiantini *et al.* (2003) published the B isotope compositions of eight geological materials that were analysed by nine laboratories, and the results showed that the interlaboratory reproducibility for some reference materials, such as B1, B2, B4, B5, B6 and B7, was not good (2 standard deviations > 3‰) and the published $\delta^{11}B$ values for AGV-2 have ~ 1.5‰ differences (Wei *et al.* 2013, Pi *et al.* 2014, Liu *et al.* 2018). Such variability is beyond the precision achieved in each individual laboratory (< 0.5‰, e.g., Foster *et al.* 2013, 2018, Wei *et al.* 2013). This may be attributed to contamination, laboratory-induced artificial fractionation (Gonfiantini *et al.* 2003) or sample heterogeneity. Therefore, to ensure data quality and avoid analytical artefacts, it is necessary to better assess the interlaboratory biases and analyse well-characterised geological reference materials. However, the database of B isotope geological reference materials is still limited and the inconsistency of the reported $\delta^{11}B$ values was not well evaluated. In this study, we report $\delta^{11}B$ values and B mass fractions for eighteen geological reference materials. These materials vary widely in matrices and include ultramafic rocks, mafic rocks, intermediate rocks, felsic rocks and sedimentary materials. All $\delta^{11}B$ results of the above reference materials are normalised to NIST SRM 951. We also evaluated the possible causes of the inconsistency of the reported B mass fractions and $\delta^{11}B$ values in previous studies and provided the recommended values for B mass fractions and $\delta^{11}B$ values of the studied materials. This work facilitates the comparison of published B isotope data and lays a foundation for using these reference materials for quality assurance.

Experimental procedure

Chemical reagents and samples

BVIII-grade hydrofluoric acid (HF), to which ~ 0.25 g l^{-1} of mannitol was added, was purified using a Savillex DST-1000 system (USA). BVIII-grade hydrochloric acid (HCl) was purified using a method similar to that for HF. Boron-free high-purity water with a resistivity of 18.2 MΩ cm was purified with a Millipore system (USA) coupled with Q-Gard® Boron that could effectively remove boron. Mannitol and ethanediol were analytical grade, and H_2O_2 was BVIII-grade. The distilled HF and HCl were diluted with B-free high-purity water to appropriate concentrations.

AGMP-1 anion exchange resin (Bio-Rad; 100–200 mesh) was used for B purification. Eighteen international

geological reference materials, including ultramafic rocks (UB-N and PCC-1), basalts (B5, W-2a, BCR-2, BHVO-2, JB-2 and JB-3), andesites (AGV-1 and JA-2), felsic rocks (B6, SDC-1, JG-1, JG-2 and JR-2) and sedimentary materials (B8, JSD-1 and SGR-1b) were analysed here. The detailed information (e.g., location and provider) of the above reference materials is described in Table 1.

Sample digestion and chromatographic separation

All digestions and separation procedures were performed in a class 100 clean hood at the State Key Laboratory of Isotope Geochemistry, Guangzhou Institute of Geochemistry, Chinese Academy of Sciences (GIG-CAS), Guangzhou, China.

Here we adopted the digestion and separation procedures reported by Wei *et al.* (2013), with some modification described by Li *et al.* (2019b). A brief description is given as follows. For each sample, a mass of approximately 100 mg (sample with B mass fraction > 8 μg g^{-1}) or 150 mg (sample with B mass fraction < 8 μg g^{-1}) was weighed into a pre-cleaned 15 ml polypropylene (PP) centrifuge tube. Next, 1.5 ml of 24 mol l^{-1} HF, 200 μl of 2% *m/m* mannitol and 150 μl of H_2O_2 were added to the tube, which was then capped tightly and placed on a hot plate at 50–55 °C for 15 days for digestion. Then, the supernatants were diluted with B-free high-purity water to an HF molarity of 3 mol l^{-1} for purification. Boron was purified using a single column loaded with AGMP-1 resin. Matrix elements were removed by 8 ml of 3 mol l^{-1} HF, 8 ml of B-free high-purity water and 48–66 ml of 0.1 mol l^{-1} HCl, and boron was then collected by 12 ml of 24 mol l^{-1} HF. Following this step, 200 μl of 2% mannitol and 100 μl of ethanediol were added to the final B eluate, and the resulting mixture was transferred into a pre-cleaned 30-ml beaker and then dried on a hot plate at 55 ± 2 °C until 100–200 μl of solution remained. Finally, the concentrated samples were redissolved with B-free high-purity water to 1.5 ml and transferred into 2 ml PP tubes for B mass fraction and isotope determination.

Boron mass fraction and isotope measurements

A 200 μl aliquot of the above-prepared solution was diluted 400 times with 2% *v/v* HNO_3 for B mass fraction measurement by using ICP-MS. Considering that the B mass fraction in the sample was determined after the separation of the boron, B single elemental standard solutions with mass fractions of 1, 5, 10, 25 and 50 ng g^{-1} were chosen to establish a standard curve and measure the B mass fraction of the unknown samples. A rhodium internal standard with a final mass fraction of 5 ng g^{-1} was added to the B single elemental standard solutions and samples for drift corrections, and the analytical precision for B mass fraction was better than 5% RSD. Unlike directly measuring the B mass fractions of samples after chromatographic separation

Table 1.
Reference materials investigated in this study are from Istituto di Geoscienze e Georisorse (IGG), Geological Society of Japan (GSJ), United States Geological Survey (USGS) and Association Nationale de la Recherche Technique (ANRT)

Sample ID	Sample type	Location	Provider
B5	Basalt	Etna Volcano (Sicily), Italy	IGG
JB-2	Basalt	Oshima volcano, Oshima, Tokyo, Japan	GSJ
JB-3	Basalt	Fuji volcano, Narusawa-mura, Yamanashi Prefecture, Japan	GSJ
BCR-2	Basalt	Columbia River Group basalt, Bridal Veil Flow Quarry, Washington, USA	USGS
BHVO-2	Basalt	Basalt Kilauea caldera, Kilauea volcano, Hawaii, USA	USGS
W-2a	Diabase	Bull Run Quarry, Fairfax county, Virginia, USA	USGS
JA-2	Andesite	Goshikidai sanukitoid, Sakaide, Kanagawa prefecture, Japan	GSJ
AGV-1	Andesite	Guano Valley, Lake County, Oregon, USA	USGS
JR-2	Rhyolite	Wada Toge obsidian, Shimosuwa-machi, Nagano Prefecture, Japan	GSJ
B6	Obsidian	Lipari Island (Aeolian Archipelago, Sicily), Italy	IGG
JG-1	Granodiorite	Sori granodiorite, Azuma-mura, Gunma Prefecture, Japan	GSJ
JG-2	Granite	Naegi granite, Hirukawa-mura, Gifu Prefecture, Japan	GSJ
SDC-1	Mica schist	Rock Creek Park, Washington, D.C, USA	USGS
B8	Clay	Pliocene clay, Montelupo (Tuscany), Italy	IGG
SGR-1b	Shale	Green River Formation, Colorado, USA	USGS
JSD-1	River sediment	Composite sample of northern region, Ibaraki Prefecture, Japan	GSJ
UB-N	Serpentinite	Col de Bagenelles (Vosges), France	ANRT
PCC-1	Peridotite	Austin Creek, California, USA	USGS

several years ago (Wei *et al.* 2013), in this experiment, the B mass fractions of samples were measured after chromatographic separation and concentration processes, which could monitor whether the B was lost during the evaporation and ensure that no artificial B isotope fractionation was introduced during chemical treatment.

The prepared B solutions were diluted with B-free high-purity water to 40–60 ng g^{-1} (^{11}B intensity of 0.4–0.5 V) at the same mass fraction as the bracketing standard (NIST SRM 951) for B isotope determination. The analytical details for mass spectrometry are presented in Li *et al.* (2019b), and a brief description is given as follows. Boron isotope compositions were determined by using a Neptune Plus MC-ICP-MS (Thermo-Fisher Scientific) with a 'wet' plasma introduction system at GIG-CAS. Instrumental mass fractionation was corrected by using the SSB technique, and the NIST SRM 951 reference solution was selected as the calibrator. The washing method after each measurement of the sample or NIST SRM 951 RM involved continuous washing with 0.3 mol l^{-1} HCl, 0.3 mol l^{-1} HCl + 0.15 mol l^{-1} HF and B-free high-purity water in sequence for 10–15 min. The ^{11}B intensity decreased from 0.4–0.5 V to ~ 3 mV after the above washing method. The isotope data were expressed in delta (δ) notation (‰):

$$\delta^{11}B_{\mathrm{SRM\,951}} = \left[\left(^{11}B/^{10}B\right)_{\mathrm{sample}} / \left(^{11}B/^{10}B\right)_{\mathrm{SRM\,951}} - 1\right] \quad (1)$$

where $(^{11}B/^{10}B)_{SRM\ 951}$ is the mean of the two bracketing calibrators, and all $^{11}B/^{10}B$ ratios in this equation were blank-corrected to account for instrumental memory effects.

Results and discussion

Yields and blanks

Previous studies have documented that chemical treatment is crucial for the accuracy of B isotope data, and poor recovery and contamination are the main problems that may hamper data quality during this process (Wei *et al.* 2013, Pi *et al.* 2014). Poor recovery of B is generally caused by loss during digestion, chromatographic separation and volatilisation. Therefore, the extraction efficiency during the digestion process and the yields of chromatographic separation were evaluated. As described in Wei *et al.* (2013), the B mass fractions in both the supernatants and the solutions dissolved from fluorite deposits by HCl and HNO_3 were determined by ICP-AES. After chromatographic separation and concentration processes, the B mass fraction in the purified B solution determined by ICP-MS was compared with that in the B solution before the chromatographic procedure was carried out. The results indicated that the B yields of digestion were $> 98\%$ and that the B yields of chromatographic separation were generally $> 99\%$. Moreover, 2% mannitol and ethanediol were used to prevent the loss of B during evaporation. Furthermore, almost all B mass fractions of the samples obtained in this study are in agreement with the literature data, which also indicates the full recovery of B during chemical treatment. In addition, to verify the purification efficiency of this chromatographic separation procedure, the final B eluate of the sample was further checked by an entire mass scan (from m/z 6 to m/z 238) on the MC-ICP-MS system, and the results showed that no significant peak of the matrices could be found except for B, argon and argon's interference masses, indicating that other matrix elements were removed effectively after chemical purification.

To reduce B contamination during chromatographic separation, ultrapure reagents with very low boron contents were used for chromatographic separation. To decrease B contamination during volatilisation, as described by Wei *et al.* (2013), the frequently used B-bearing materials in the air filters of the clean bench were replaced with B-free materials such as polypropylene (PP). Further, each beaker that contained the final B eluate was covered with a pre-cleaned PP beaker, with only a narrow gap for the vapour to exit. In addition, to prevent potential contamination by the PP tube, the B mass fractions and isotope compositions of the prepared B solution were determined as soon as possible. After the above modifications, the blanks for the whole procedure, including digestion, chromatographic separation and evaporation, were repeatedly tested by following all the steps but without digesting and loading any sample, and the results showed that the whole procedural blanks of B were less than 6 ng. Except for JG-2 and BHVO-2, these blanks were negligible ($< 1\%$) compared with the amount of B of other samples loaded on the column. As such, our method can purify boron from rock matrices efficiently and achieves low blank and high recovery during chemical treatment so that no artificial B isotope fractionation was introduced into our purification process.

Evaluating the precision of boron isotope measurements

The precision of B isotope measurements was evaluated by repeatedly measuring the B isotope composition of the calibration solution NIST SRM 951. The intermediate measurement precision of $\delta^{11}B$ for NIST SRM 951 was better than 0.5‰ (2s) over 1 year (Figure 1).

The robustness of the overall B isotope analytical procedure is evaluated by repeated measurements of five

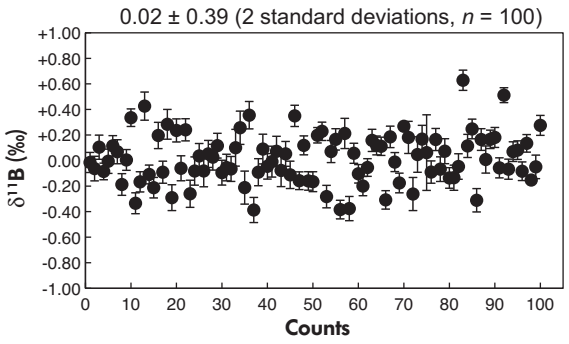

Figure 1. Plot illustrating the intermediate measurement precision of δ^{11}B over a long-term (> 1 year) period for NIST SRM 951.

reference materials (i.e., B5, JB-2, JB-3, B6 and JR-2). The analytical results of the above reference materials, together with the compiled published results, are listed in Table 2. The compiled δ^{11}B values of the analysed samples were the mean value calculated from all available literature data (Appendix A). The measured δ^{11}B values of the five reference materials are as follows: B5 = -4.43 ± 0.8‰ (2*s*, *n* = 5), JB-2 = +7.22 ± 0.45‰ (2*s*, *n* = 5), JB-3 = +6.75 ± 0.41‰ (2*s*, *n* = 5), B6 = -2.71 ± 0.29‰ (2*s*, *n* = 5) and JR-2 = 3.35 ± 0.51‰ (2*s*, *n* = 8). The δ^{11}B values of JB-3 and B6 obtained in this study are consistent with the results reported in Li *et al.* (2019b) but they are ~ 1‰ higher and lower than the results reported in Wei *et al.* (2013), respectively, which may be caused by different matrix effects on these measurements compared with those carried out 8 years ago (Li *et al.* 2019b). The modified B isotope measurement procedure in Li *et al.* (2019b) improves the washing process and more strictly matches the acidity and concentration between the standard and the samples (Chen *et al.* 2016), which helps improve the stability during B isotope measurement. Besides, as shown in Figure 2 and Table 2, the measured δ^{11}B values of the above reference materials are consistent with almost all published results, which verifies the robustness of our overall B isotope analytical procedure.

Boron mass fractions and isotope compositions of geological reference materials

We report our measurement results in Table 2, for B mass fractions and $\delta^{11}B_{SRM\ 951}$ values in eighteen geological reference materials. We also report in Table 2 mean literature values, when available, and, in columns 'Combined', the mean of our results and the individual literature values detailed in Appendix A. These 'Combined' data could serve as reference values in future studies.

Our results on B mass fractions in the eighteen reference materials range from 2.37 to 158 μg g^{-1}. They are all in good agreement with the literature data (Table 2, Appendix A and Figure 3), except for JG-2, UB-N and PCC-1. For JG-2, our measured B mass fractions are 2.37 ± 0.14 μg g^{-1}, which is similar to most literature data (1.86 ± 0.39 μg g^{-1}; compiled by Imai *et al.* 1995, D'Orazio 1999, Romer *et al.* 2014) but lower than the reported values (6.80 ± 0.90 μg g^{-1}) in Harvey *et al.* (1996). These higher values reported by Harvey *et al.* (1996) were measured by PGAA, and the B mass fraction obtained by this method may be greatly different from the published results (obtained by ICP-AES or ICP-MS) when the matrices of the samples do not match with those of the reference materials. A similar discrepancy was also reported by Gméling *et al.* (2005) and Leeman *et al.* (2017; e.g., the B contents of JR-1 and/or JR-2 measured by PGAA were higher than the published results obtained by other methods). Therefore, for JG-2 the combined value of 1.99 ± 0.60 μg g^{-1} was obtained by averaging our result with all literature values except the highest. For UB-N, our measured B mass fractions are 158 ± 7.81 μg g^{-1}, which is consistent with the published results reported by D'Orazio (1999; 157 μg g^{-1}) and by Govindaraju (1995; 140 ± 34.6 μg g^{-1}), but higher than the literature data reported by Govindaraju (1994; 140 μg g^{-1}) and Peters and Pettke (2017; 135 ± 2.97 μg g^{-1}). This discrepancy may be caused by experimental errors introduced by chemical treatment because serpentinite rocks are very difficult to dissolve. For PCC-1, the mean mass fraction of 1.70 μg g^{-1} reported by Govindaraju (1994) was compiled from the reported values (Gordon *et al.* 1979, Gladney *et al.* 1984, Higgins 1984, Anderson *et al.* 1985, Walsh 1985) except the three highest values in Gladney *et al.* (1991). Other three values were 4.69 ± 0.33 μg g^{-1} (Mortier *et al.* 1982), 6.0 μg g^{-1} (Thompson *et al.* 1970) and 12.8 μg g^{-1} [published data in Flanagan (1969)], respectively. The B mass fraction of AGV-1 (13.8 μg g^{-1}) reported in Flanagan (1969) was also higher than the compile values of AGV-1 (7.97 ± 0.31 μg g^{-1}), which may indicate that the value of 12.8 for PCC-1 reported in Flanagan (1969) was higher than the real value. Considering that most reported values measured by PGAA or AES do not provide the uncertainty of the measurement, and the reproducibility of these results measured by PGAA or AES is thus difficult to evaluate, it is difficult to clarify the discrepancy of B mass fraction for PCC-1. Our measured B mass fractions of PCC-1 are 4.41 ± 0.64 μg g^{-1}, which is in agreement with the values (4.69 ± 0.33 μg g^{-1}) measured by charged particle activation analysis (Mortier *et al.* 1982). Such analytical results seem to indicate that the mass fraction of this sample is homogeneous but more investigations on PCC-1 are still required to further verify whether it is homogeneous.

Table 2.
Boron mass fraction and isotopic data for a selected range of geological reference materials

Material	Type	B mass fraction data ± 1*s* (μg g^{-1})			$\delta^{11}B_{SRM\ 951}$ data ± 1*s* (‰)		
		This work [a]	Literature [b]	Combined [c]	This work [a]	Literature [b]	Combined [c]
B5	Basalt	10.0 ± 0.4 (*n* = 3)	9.74 ± 1.09	9.76 ± 1.05 (*n* = 14)	-4.43 ± 0.40 (*n* = 5)	-4.02 ± 0.37	-4.06 ± 0.37 (*n* = 12)
JB-2	Basalt	29.5 ± 0.9 (*n* = 3)	30.0 ± 0.9	30.0 ± 0.9 (*n* = 20)	+7.22 ± 0.23 (*n* = 5)	+7.21 ± 0.41	+7.27 ± 0.29 (*n* = 26)
JB-3	Basalt	20.0 ± 0.8 (*n* = 3)	19.4 ± 1.8	19.4 ± 1.7 (*n* = 19)	+6.75 ± 0.21 (*n* = 5)	+6.32 ± 0.47	+6.36 ± 0.46 (*n* = 11)
BCR-2	Basalt	4.40 ± 0.13 (*n* = 3)	4.96 ± 1.55	4.30 ± 0.25 (*n* = 5)	-5.70 ± 0.35 (*n* = 7)	-5.92 ± 0.02	-5.84 ± 0.13 (*n* = 3)
BHVO-2	Basalt	2.62 ± 0.03 (*n* = 3)	2.95 ± 0.14	2.89 ± 0.19 (*n* = 6)	-2.38 ± 0.47 (*n* = 6)	-1.16 ± 0.65	-1.56 ± 0.84 (*n* = 3)
W-2a	Diabase	14.0 ± 0.1 (*n* = 2)	–	14.0 ± 0.1	+9.09 ± 0.61 (*n* = 6)	–	+9.09 ± 0.61
JA-2	Andesite	23.8 ± 0.6 (*n* = 3)	20.8 ± 0.9	21.0 ± 1.3 (*n* = 11)	-7.73 ± 0.24 (*n* = 6)	-9.30 ± 0.45	-8.52 ± 1.11 (*n* = 2)
AGV-1	Andesite	8.32 ± 0.18 (*n* = 3)	7.97 ± 0.15	8.03 ± 0.20 (*n* = 6)	-4.84 ± 0.29 (*n* = 6)	–	-4.84 ± 0.29
JR-2	Rhyolite	146 ± 3 (*n* = 3)	154 ± 16	151 ± 15 (*n* = 8)	+3.35 ± 0.26 (*n* = 8)	+2.77 ± 0.21	+2.85 ± 0.29 (*n* = 7)
B6	Obsidian	207 ± 4 (*n* = 3)	206 ± 14	203 ± 8 (*n* = 12)	-2.71 ± 0.14 (*n* = 5)	-2.55 ± 0.73	-2.56 ± 0.69 (*n* = 10)
JG-1	Granodiorite	5.73 ± 0.08 (*n* = 3)	6.30 ± 0.49	6.16 ± 0.49 (*n* = 4)	-10.30 ± 0.15 (*n* = 6)	–	-10.30 ± 0.15
JG-2	Granite	2.37 ± 0.07 (*n* = 3)	3.10 ± 2.48	1.99 ± 0.30 (*n* = 4)	-11.87 ± 0.82 (*n* = 6)	-12.23 ± 0.40	-12.05 ± 0.25 (*n* = 2)
SDC-1	Mica schist	12.2 ± 0.4 (*n* = 3)	12.9 ± 0.1	12.7 ± 0.4 (*n* = 3)	-5.93 ± 0.40 (*n* = 7)	-5.50 ± 0.35	-5.72 ± 0.30 (*n* = 2)
B8	Clay	100 ± 2 (*n* = 3)	98.6 ± 7.4	98.8 ± 7.2 (*n* = 12)	-5.28 ± 0.25 (*n* = 6)	-5.06 ± 0.38	-5.09 ± 0.36 (*n* = 10)
SGR-1b	Shale	48.6 ± 1.3 (*n* = 3)	–	48.6 ± 1.3	-28.85 ± 0.19 (*n* = 6)	–	-28.85 ± 0.19
JSD-1	River sediment	7.96 ± 0.19 (*n* = 3)	–	7.96 ± 0.19	-1.97 ± 0.20 (*n* = 6)	–	-1.97 ± 0.20
UB-N	Serpentinite	158 ± 4 (*n* = 2)	143 ± 10	146 ± 11 (*n* = 5)	+10.47 ± 0.26 (*n* = 6)	+13.1 ± 0.21	+11.79 ± 1.86 (*n* = 2)
PCC-1	Peridotite	4.40 ± 0.32 (*n* = 3)	3.99 ± 3.95	4.03 ± 3.70 (*n* = 9)	+8.19 ± 0.13 (*n* = 6)	–	+8.19 ± 0.13

Three categories of data are reported: results from this work, values corresponding to a compilation of literature data and values corresponding to a combination of results from this work and a selection of literature data (for calculation details, see footnotes and Appendix A).

For mass fraction data, values marked with * in Appendix A correspond to the highest values reported by Adam *et al.* (2014; BCR-2), Kasemann *et al.* (2001; JR-2), Gonfiantini *et al.* (2003; B6) and Harvey *et al.* (1996; JG-2).

For isotopic data, only the values reported by Leeman *et al.* (2004) for JB-2 were marked with * in Appendix A.

[a] Values in 'This work' columns are the means of the results in this study.

[b] Values in 'Literature' columns are the values reported as 'Mean' in Appendix A.

[c] Values in 'Combined' columns are means between results from this work and a selection of the literature values described in Appendix A. In Appendix A, values marked with * are not taken into account for the calculations 'Combined'.

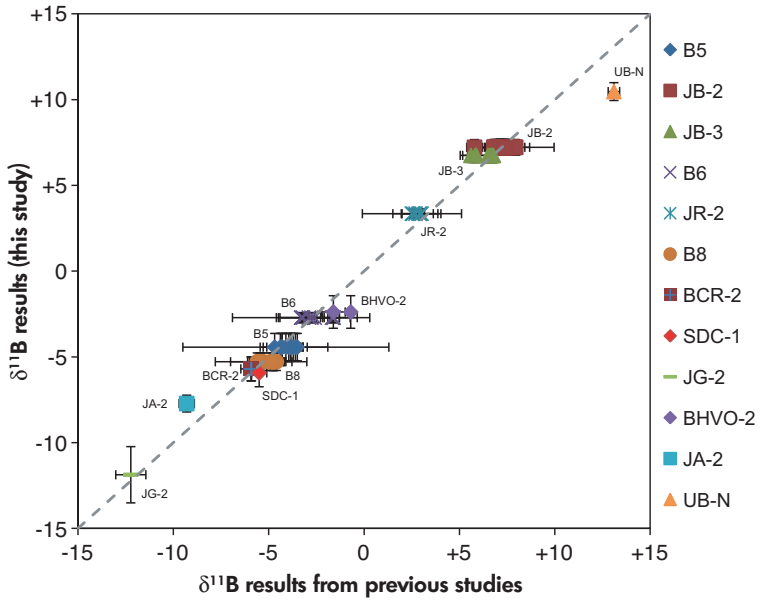

Figure 2. Plot of δ^{11}B results determined in this study vs. literature δ^{11}B values.

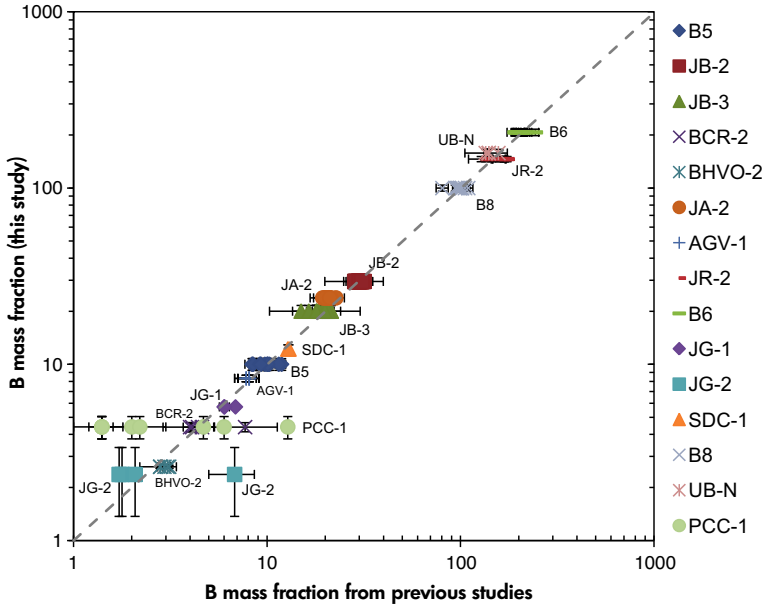

Figure 3. Log-log plot of B mass fractions determined in this study versus literature B mass fractions.

For each material, we replicated our B isotopic measurements at least three times on samples prepared separately. Our results for δ^{11}B on all materials range from -28.85 to +10.47‰ (Figure 4). Besides the measured δ^{11}B values of the five reference materials (i.e., B5, JB-2, JB-3, B6 and JR-2) shown above (*Evaluating the precision of B isotope measurements*), the measured δ^{11}B values of BCR-2 (-5.70 ± 0.70‰, n = 7), SDC-1 (-5.93 ± 0.81‰, n = 6), JG-2 (-11.87 ± 1.64‰, n = 6) and B8 (-5.28 ± 0.51‰, n = 6) in this study are also consistent with published results (Figure 2). Unlike the inconsistent δ^{11}B results between laboratories reported by Gonfiantini *et al.* (2003), the δ^{11}B results for B5, B6 and B8 reported in most laboratories were consistent in the last two decades (Appendix A). This evolution is possibly the confirmation that the inconsistencies underlined by Gonfiantini *et al.* (2003) were due to problems during sample preparation and at the stage of extracting B from sample matrices in particular.

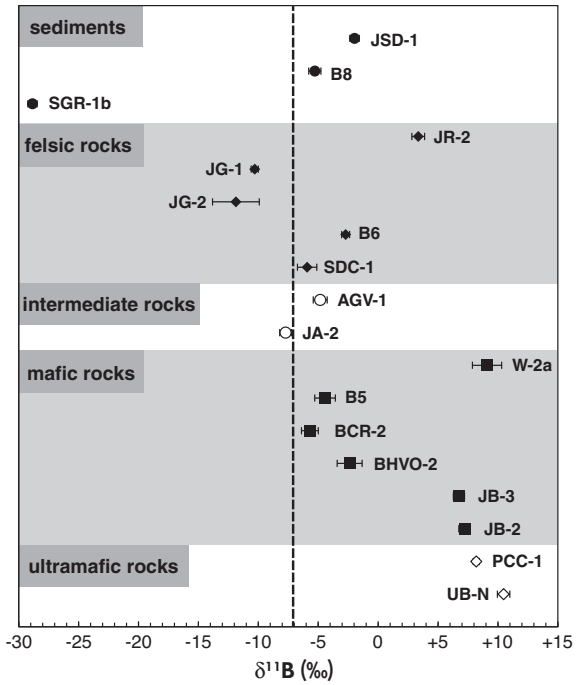

Figure 4. δ^{11}B values of the eighteen geological reference materials, which are normalised to NIST SRM 951 (δ^{11}B = 0‰). The vertical black dotted line represents the δ^{11}B value of the Earth's mantle (δ^{11}B = -7.1‰).

The spread of δ^{11}B values of JG-2 obtained in this study is a bit wider than other studied materials, which may be caused by its low B content: assuming the B isotope composition of the blank was 50‰ different from that of the respective sample (based on our determined B isotope compositions of procedural blanks), a 6 ng B blank affecting a 355 ng B sample (B amount of JG-2) caused a shift of about 0.85‰ in δ^{11}B value, while a 6 ng B blank affecting other samples with higher B content (B mass fraction > 4.40 μg g^{-1}) caused a shift of < 0.45‰ in δ^{11}B value. The measured δ^{11}B values of BHVO-2 are -2.38 ± 0.95‰ (2*s*, *n* = 6), which is (~ 1.50‰) lower than the δ^{11}B values reported by Wei *et al.* (2013) but is consistent with the value reported by Liu *et al.* (2018). The reason for this discrepancy may be the low B content of BHVO-2 (2.62 ± 0.05 μg g^{-1}). As mentioned above, the δ^{11}B analytical results of samples with lower B content are more influenced by the B blank.

The measured δ^{11}B values of JA-2 are -7.72 ± 0.49‰ (2*s*, *n* = 6), which is (~ 1.50‰) higher than the δ^{11}B values reported by Wei *et al.* (2013) and the δ^{11}B value of UB-N is +10.47 ± 0.52‰ (2*s*, *n* = 5), which is (~ 2.50‰) lower than the δ^{11}B values reported by Wei *et al.* (2013). Considering that the B contents of JA-2 and UB-N are relatively high, the influence of the blank should be negligible (< 0.12‰). These discrepancies may be caused by the different matrix effect on this measurement compared with those carried out several years ago and/or the B isotope compositions of JA-2 and UB-N may be heterogeneous, but more investigations on JA-2 and UB-N are still required to further verify whether they are heterogeneous.

The new δ^{11}B results of six reference materials are as follows: W-2a = +9.09 ± 1.22‰ (2*s*, *n* = 6), AGV-1 = -4.84 ± 0.58‰ (2*s*, *n* = 6), JG-1 = -10.30 ± 0.30‰ (2*s*, *n* = 6), SGR-1b = -28.85 ± 0.38‰ (2*s*, *n* = 6), JSD-1 = -1.97 ± 0.39‰ (2*s*, *n* = 6) and PCC-1 = +8.19 ± 0.26‰ (2*s*, *n* = 6). The new δ^{11}B results of the above reference materials presented here and the recommended δ^{11}B values of the other twelve reference materials (reported in Table 2 in the columns 'Combined') could serve as reference for quality assurance and future comparisons.

Conclusions

The reference materials analysed in this study cover a wide range of matrices, with igneous rocks, and from ultramafic rocks to felsic rocks and sedimentary materials. Significant discrepancy of δ^{11}B values (1.5–2.5‰) in JA-2 and UB-N suggests that the B isotope compositions of these two reference materials may be heterogeneous and more investigations on JA-2 and UB-N are still required to further ascertain their δ^{11}B values, and using the above reference materials for quality control should thus be approached with caution.

Acknowledgements

The authors thank Xianglin Tu of the State key Laboratory of Isotope Geochemistry, GIG-CAS for his assistance in running the Thermo Element ICP-MS. This work was supported by the National Natural Science Foundation of China (Grant No. 41991325), the Strategic Priority Research Program (B) of the Chinese Academy of Sciences (Grant No. XDB18000000), Fundamental and Applied Fundamental Research Major Program of Guangdong Province (Grant No. 2019B030302013), Key Special Project for Introduced Talents Team of Southern Marine Science and Engineering Guangdong Laboratory (Guangzhou; Grant No. GML2019ZD0308) and the Natural Science Foundation of Guangdong Province of China (2021A1515017789). This paper is contribution No. IS-3035 from GIG-CAS.

Data availability statement

We are willing to share our research data including, but not limited to: raw data, processed data, software, algorithms, protocols, methods, materials after manuscript acceptance.

References

Adam J., Locmelis M., Afonso J.C., Rushmer T. and Fiorentini M.L. (2014)
The capacity of hydrous fluids to transport and fractionate incompatible elements and metals within the Earth's mantle. **Geochemistry, Geophysics, Geosystems**, 15, 2241–2253.

Anderson D.L., Sun Y., Failey M.P. and Zoller W.H. (1985)
Neutron-capture prompt gamma-ray multi-element analysis of twenty-two geochemical reference standards. **Geostandards Newsletter**, 9, 219–228.

Berryman E.J., Kutzschbach M., Trumbull R.B., Meixner A., van Hinsberg V., Kasemann S.A. and Franz G. (2017)
Tourmaline as a petrogenetic indicator in the Pfitsch Formation, western Tauern Window, eastern Alps. **Lithos**, 284–285, 138–155.

Boschi C., Bonatti E., Ligi M., Brunelli D., Cipriani A., Dallai L., D'Orazio M., Früh-Green G.L., Tonarini S., Barnes J.D. and Bedini R.M. (2013)
Serpentinization of mantle peridotites along an uplifted lithospheric section, Mid Atlantic Ridge at 11° N. **Lithos**, 178, 3–23.

Boschi C., Dini A., Früh-Green G.L. and Kelley D.S. (2008)
Isotopic and element exchange during serpentinization and metasomatism at the Atlantis Massif (MAR 30°N): Insights from B and Sr isotope data. **Geochimica et Cosmochimica Acta**, 72, 1801–1823.

Chen X.F., D'Olivo J.P., Wei G.J. and McCulloch M. (2019)
Anthropogenic ocean warming and acidification recorded by Sr/Ca, Li/Mg, $\delta^{11}B$ and B/Ca in *Porites* coral from the Kimberley region of northwestern Australia. **Palaeogeography Palaeoclimatology Palaeoecology**, 528, 50–59.

Chen X.F., Zhang L., Wei G.J. and Ma J.L. (2016)
Matrix effects and mass bias caused by inorganic acids on boron isotope determination by multi-collector ICP-MS. **Journal of Analytical Atomic Spectrometry**, 31, 2410–2417.

Chetelat B., Liu C.Q., Gaillardet J., Wang Q.L., Zhao Z.Q., Liang C.S. and Xiao Y.K. (2009)
Boron isotopes geochemistry of the Changjiang basin rivers. **Geochimica et Cosmochimica Acta**, 73, 6084–6097.

D'Orazio M. (1999)
Boron determination in twenty one silicate rock reference materials by isotope dilution ICP-MS. **Geostandards Newsletter: The Journal of Geostandards and Geoanalysis**, 23, 21–29.

Devulder V., Degryse P. and Vanhaecke F. (2013)
Development of a novel method for unraveling the origin of natron flux used in Roman glass production based on B isotopic analysis via multicollector inductively coupled plasma-mass spectrometry. **Analytical Chemistry**, 85, 12077–12084.

Devulder V., Gerdes A., Vanhaecke F. and Degryse P. (2015)
Validation of the determination of the B isotopic composition in Roman glasses with laser ablation multi-collector inductively coupled plasma-mass spectrometry. **Spectrochimica Acta Part B**, 105, 116–120.

Deyhle A. (2001)
Improvements of boron isotope analysis by positive thermal ionization mass spectrometry using static multicollection of $Cs_2BO_2^+$ ions. **International Journal of Mass Spectrometry**, 206, 79–89.

Dreyer B.M., Morris J.D. and Gill J.B. (2010)
Incorporation of subducted slab-derived sediment and fluid in arc magmas: B-Be-^{10}Be-Nd systematics of the Kurile convergent margin, Russia. **Journal of Petrology**, 51, 1761–1782.

Dyar M.D., Wiedenbeck M., Robertson D., Cross L.R., Delaney J.S., Ferguson K., Francis C.A., Grew E.S., Guidotti C.V., Hervig R.L., Hughes J.M., Husler J., Leeman W., McGuire A.V., Rhede D., Rothe H., Paul R.L., Richards I. and Yates M. (2001)
Reference minerals for the microanalysis of light elements. **Geostandards Newsletter: The Journal of Geostandards and Geoanalysis**, 25, 441–463.

Ercolani C., Lemarchand D. and Dosseto A. (2019)
Insights on catchment-wide weathering regimes from boron isotopes in riverine material. **Geochimica et Cosmochimica Acta**, 261, 35–55.

Flanagan F.J. (1969)
U.S. Geological Survey standards – II. First compilation of data for the new U.S.G.S. rocks. **Geochimica et Cosmochimica Acta**, 33, 81–120.

Foster G.L., Hönisch B., Paris G., Dwyer G.S., Rae J.W.B., Elliott T., Gaillardet J., Hemming N.G., Louvat P. and Vengosh A. (2013)
Interlaboratory comparison of boron isotope analyses of boric acid, seawater and marine $CaCO_3$ by MC-ICP-MS and NTIMS. **Chemical Geology**, 358, 1–14.

Foster G.L., Marschall H.R. and Palmer M.R. (2018).
Boron isotope analysis of geologic materials. **In: Marschall H.R. and Foster G.L. (eds), Boron isotopes – The fifth element. Advances in isotope geochemistry. Springer** (Heidelberg), 13–31.

references

Garda G.M., Trumbull R.B., Bejavskis P. and Wiedenbeck M. (2009)
Boron isotope composition of tourmalinite and vein tourmalines associated with gold mineralization, Serra do Itaberaba Group, central Ribeira Belt, SE Brazil. Chemical Geology, 264, 207–220.

Genske F.S., Turner S.P., Beier C., Chu M.-F., Tonarini S., Pearson N.J. and Haase K.M. (2014)
Lithium and boron isotope systematics in lavas from the Azores islands reveal crustal assimilation. Chemical Geology, 373, 27–36.

Gladney E.S., Curtis D.B. and Perrin D.R. (1984)
Determination of boron in 35 international geochemical reference materials by thermal neutron capture prompt gamma-ray spectrometry. Geostandards Newsletter, 8, 43–46.

Gladney E.S., Jones E.A., Nickell E.J. and Roelandts I. (1991)
1988 compilation of elemental concentration data for USGS DTS-1, G-1, PCC-1 and W-1. Geostandards Newsletter, 15, 199–396.

Gméling K., Harangi S. and Kasztovszky Z. (2005)
Boron and chlorine concentration of volcanic rocks: An application of prompt gamma activation analysis. Journal of Radioanalytical and Nuclear Chemistry, 265, 201–212.

Gonfiantini R., Tonarini S., Groning M., Adorni-Braccesi A., Al-Ammar A.S., Astner M., Bachler S., Barnes R.M., Bassett R.L., Cocherie A., Deyhle A., Dini A., Ferrara G., Gaillardet J., Grimm J., Guerrot C., Krahenbuhl U., Layne G., Lemarchand D., Meixner A., Northington D.J., Pennisi M., Reitznerova E., Rodushkin I., Sugiura N., Surberg R., Tonn S., Wiedenbeck M., Wunderli S., Xiao Y.K. and Zack T. (2003)
Intercomparison of boron isotope and concentration measurements. Part II: Evaluation of results. Geostandards Newsletter: The Journal of Geostandards and Geoanalysis, 27, 41–57.

Gordon G.E., Zoller W.H. and Walters W.B. (1979)
Non-destructive determination of trace-element concentrations. Technical Report ORO-5173-008. Department of Chemistry, Maryland University (College Park).

Govindaraju K. (1994)
1994 compilation of working values and sample description for 383 geostandards. Geostandards Newsletter, 18 (Special Issue), 158pp.

Govindaraju K. (1995)
1995 working values with confidence limits for twenty-six CRPG, ANRT and IWG-GIT geostandards. Geostandards Newsletter, 19 (Special Issue), 32pp.

Gurenko A.A., Veksler I.V., Meixner A., Thomas R., Dorfman A.M. and Dingwell D.B. (2005)
Matrix effect and partitioning of boron isotopes between immiscible Si-rich and B-rich liquids in the Si–Al–B–Ca–Na–O system: A SIMS study of glasses quenched from centrifuge experiments. Chemical Geology, 222, 268–280.

Hansen C.T., Meixner A., Kasemann S.A. and Bach W. (2017)
New insight on Li and B isotope fractionation during serpentinization derived from batch reaction investigations. Geochimica et Cosmochimica Acta, 217, 51–79.

Harvey J., Garrido C.J., Savov I., Agostini S., Padrón-Navarta J.A., Marchesi C., López S.-V. and Gómez-Pugnaire M.T. (2014)
^{11}B-rich fluids in subduction zones: The role of antigorite dehydration in subducting slabs and boron isotope heterogeneity in the mantle. Chemical Geology, 376, 20–30.

Harvey P.K., Lovell M.A., Brewer T.S., Locke J. and Mansley E. (1996)
Measurement of thermal neutron absorption cross section in selected geochemical reference materials. Geostandards Newsletter, 20, 79–85.

Higgins M. (1984)
Abundance of boron in international geochemical standards by prompt-gamma neutron-activation analysis. Geostandards Newsletter, 8, 31–34.

Hou K., Li Y., Xiao Y., Liu F. and Tian Y. (2010)
In situ boron isotope measurements of natural geological materials by LA-MC-ICP-MS. Chinese Science Bulletin, 55, 3305–3311.

Hu Z. and Gao S. (2008)
Upper crustal abundances of trace elements: A revision and update. Chemical Geology, 253, 205–221.

Imai N., Terashima S., Itoh S. and Ando A. (1995)
1994 Compilation of analytical data for minor and trace elements in seventeen GSJ geochemical reference samples, "Igneous rock series". Geostandards Newsletter, 19, 135–213.

Ishikawa T., Tera F. and Nakazawa T. (2001)
Boron isotope and trace element systematics of the three volcanic zones in the Kamchatka arc. Geochimica et Cosmochimica Acta, 65, 4523–4537.

Jochum K.P., Weis U., Schwager B., Stoll B., Wilson S.A., Haug G.H., Andreae M.O. and Enzweiler J. (2016)
Reference values following ISO guidelines for frequently requested rock reference materials. Geostandards and Geoanalytical Research, 40, 333–350.

Kasemann S., Meixner A., Rocholl A., Vennemann T., Rosner M., Schmitt A.K. and Wiedenbeck M. (2001)
Boron and oxygen isotope composition of certified reference materials NIST SRM 610/612 and reference materials JB-2 and JR-2. Geostandards Newsletter: The Journal of Geostandards and Geoanalysis, 25, 405–416.

Kimura J.-I., Chang Q., Ishikawa T. and Tsujimori T. (2016)
Influence of laser parameters on isotope fractionation and optimisation of lithium and boron isotope ratio measurements using laser ablation-multiple Faraday collector-inductively coupled plasma-mass spectrometry. Journal of Analytical Atomic Spectrometry, 31, 2305–2320.

Kiss E. (1988)
Ion-exchange separation and spectrophotometric determination of boron in geological materials. Analytica Chimica Acta, 211, 243–256.

references

Kitagawa H., Kobayashi K., Makishima A. and Nakamura E. (2008)
Multiple pulses of the mantle plume: Evidence from Tertiary Icelandic lavas. Journal of Petrology, 49, 1365–1396.

Kurosawa M., Shima K., Ishii S. and Sasa K. (2006)
Trace element analysis of fused whole-rock glasses by laser ablation-ICP-MS and PIXE. Geostandards and Geoanalytical Research, 30, 17–30.

Lambert-Smith J.S., Rocholl A., Treloar P.J. and Lawrence D.M. (2016)
Discriminating fluid source regions in orogenic gold deposits using B-isotopes. Geochimica et Cosmochimica Acta, 194, 57–76.

Le Fevre B. and Ottolini L. (2006)
Preparation of reference glasses for *in-situ* analysis of lithium and boron. Microchimica Acta, 155, 189–194.

le Roux P.J., Shirey S.B., Benton L., Hauri E.H. and Mock T.D. (2004)
In situ, multiple-multiplier, laser ablation ICP-MS measurement of boron isotopic composition ($\delta^{11}B$) at the nanogram level. Chemical Geology, 203, 123–138.

Leeman W.P. and Tonarini S. (2001)
Boron isotopic analysis of proposed borosilicate mineral reference samples. Geostandards Newsletter: The Journal of Geostandards and Geoanalysis, 25, 399–403.

Leeman W.P., Tonarini S., Chan L.H. and Borg L.E. (2004)
Boron and lithium isotopic variations in a hot subduction zone – The southern Washington Cascades. Chemical Geology, 212, 101–124.

Leeman W.P., Tonarini S. and Turner S. (2017)
Boron isotope variations in Tonga-Kermadec-New Zealand arc lavas: Implications for the origin of subduction components and mantle influences. Geochemistry, Geophysics, Geosystems, 18, 1126–1162.

Lemarchand D., Cividini D., Turpault M.P. and Chabaux F. (2012)
Boron isotopes in different grain size fractions: Exploring past and present water–rock interactions from two soil profiles (Strengbach, Vosges Mountains). Geochimica et Cosmochimica Acta, 98, 78–93.

Lemarchand D. and Gaillardet J. (2006)
Transient features of the erosion of shales in the Mackenzie basin (Canada), evidences from boron isotopes. Earth and Planetary Science Letters, 245, 174–189.

Li H.-Y., Li J., Ryan J.G., Li X., Zhao R.-P., Ma L. and Xu Y.-G. (2019a)
Molybdenum and boron isotope evidence for fluid-fluxed melting of intraplate upper mantle beneath the eastern North China Craton. Earth and Planetary Science Letters, 520, 105–114.

Li H.-Y., Zhou Z., Ryan J.G., Wei G.-J. and Xu Y.-G. (2016)
Boron isotopes reveal multiple metasomatic events in the mantle beneath the eastern North China Craton. Geochimica et Cosmochimica Acta, 194, 77–90.

Li X., Li H.-Y., Ryan J.G., Wei G.-J., Zhang L., Li N.-B., Huang X.-L. and Xu Y.-G. (2019b)
High-precision measurement of B isotopes on low-boron oceanic volcanic rock samples via MC-ICP-MS: Evaluating acid leaching effects on boron isotope compositions, and B isotopic variability in depleted oceanic basalts. Chemical Geology, 505, 76–85.

Liu Y.-H., Huang K.-F. and Lee D.-C. (2018)
Precise and accurate boron and lithium isotopic determinations for small sample-size geological materials by MC-ICP-MS. Journal of Analytical Atomic Spectrometry, 33, 846–855.

Lu Y., Makishima A. and Nakamura E. (2007)
Coprecipitation of Ti, Mo, Sn and Sb with fluorides and application to determination of B, Ti, Zr, Nb, Mo, Sn, Sb, Hf and Ta by ICP-MS. Chemical Geology, 236, 13–26.

Mao H.-R., Liu C.-Q. and Zhao Z.-Q. (2019)
Source and evolution of dissolved boron in rivers: Insights from boron isotope signatures of end-members and model of boron isotopes during weathering processes. Earth-Science Reviews, 190, 439–459.

Marschall H.R. and Foster G.L. (2018).
Boron isotopes in the Earth and planetary sciences – History and background. In: Marschall H.R. and Foster G.L. (eds), Boron isotopes – the fifth element. Advances in isotope geochemistry. Springer (Heidelberg), 1–11.

Marschall H.R., Wanless V.D., Shimizu N., Pogge von Strandmann P.A.E., Elliott T. and Monteleone B.D. (2017)
The boron and lithium isotopic composition of mid-ocean ridge basalts and the mantle. Geochimica et Cosmochimica Acta, 207, 102–138.

Menard G., Vlastélic I., Ionov D.A., Rose-Koga E.F., Piro J.L. and Pin C. (2013)
Precise and accurate determination of boron concentration in silicate rocks by direct isotope dilution ICP-MS: Insights into the B budget of the mantle and B behavior in magmatic systems. Chemical Geology, 354, 139–149.

Michel A., Noireaux J. and Tharaud M. (2015)
Determination of boron concentration in geochemical reference materials extracted by pyrohydrolysis and measured by ICP-MS. Geostandards and Geoanalytical Research, 39, 489–495.

Mohan M.R., Kamber B.S. and Piercey S.J. (2008)
Boron and arsenic in highly evolved Archean felsic rocks: Implications for Archean subduction processes. Earth and Planetary Science Letters, 274, 479–488.

Mori L., Gómez-Tuena A., Cai Y. and Goldstein S.L. (2007)
Effects of prolonged flat subduction on the Miocene magmatic record of the central Trans-Mexican Volcanic Belt. Chemical Geology, 244, 452–473.

references

Mortier R., Vandecasteele C., Hertogen J. and Hoste J. (1982)
The determination of boron in rocks by deuteron activation analysis. Journal of Radioanalytical Chemistry, 71, 189–198.

Nakamura E., Ishikawa T., Birck J.-L. and Allègre C.J. (1992)
Precise boron isotopic analysis of natural rock samples using a boron-mannitol complex. Chemical Geology, 94, 193–204.

Pal D.C., Trumbull R.B. and Wiedenbeck M. (2010)
Chemical and boron isotope compositions of tourmaline from the Jaduguda U(-Cu-Fe) deposit, Singhbhum shear zone, India: Implications for the sources and evolution of mineralizing fluids. Chemical Geology, 277, 245–260.

Pennisi M., Bianchini G., Kloppmann W. and Muti A. (2009)
Chemical and isotopic (B, Sr) composition of alluvial sediments as archive of a past hydrothermal outflow. Chemical Geology, 266, 114–125.

Peters D. and Pettke T. (2017)
Evaluation of major to ultra trace element bulk rock chemical analysis of nanoparticulate pressed powder pellets by LA-ICP-MS. Geostandards and Geoanalytical Research, 41, 5–28.

Pi J.-L., You C.-F. and Chung C.-S. (2014)
Micro-sublimation separation of boron in rock samples for isotopic measurement by MC-ICP-MS. Journal of Analytical Atomic Spectrometry, 29, 861–867.

Pi J.-L., You C.-F. and Wang K.-L. (2016)
The influence of Ryukyu subduction on magma genesis in the Northern Taiwan Volcanic Zone and Middle Okinawa Trough – Evidence from boron isotopes. Lithos, 260, 242–252.

Rae J.W.B., Foster G.L., Schmidt D.N. and Elliott T. (2011)
Boron isotopes and B/Ca in benthic foraminifera: Proxies for the deep ocean carbonate system. Earth and Planetary Science Letters, 302, 403–413.

Raffone N., Ottolini L., Tonarini S., Gianelli G. and Fridleifsson G.Ó. (2008)
A SIMS study of lithium, boron and chlorine in basalts from Reykjanes (southwestern Iceland). Microchimica Acta, 161, 307–312.

Raitzsch M., Bijma J., Benthien A., Richter K.-U., Steinhoefel G. and Kucera M. (2018)
Boron isotope-based seasonal paleo-pH reconstruction for the southeast Atlantic – A multispecies approach using habitat preference of planktonic foraminifera. Earth and Planetary Science Letters, 487, 138–150.

Rasbury E.T. and Hemming N.G. (2017)
Boron isotopes: A "paleo-pH meter" for tracking ancient atmospheric CO_2. Elements, 13, 243–248.

Romer R.L., Meixner A. and Hahne K. (2014)
Lithium and boron isotopic composition of sedimentary rocks – the role of source history and depositional environment: A 250 Ma record from the Cadomian orogeny to the Variscan orogeny. Gondwana Research, 26, 1093–1110.

Rose E.F., Chaussidon M. and France-Lanord C. (2000)
Fractionation of Boron isotopes during erosion processes: The example of Himalayan rivers. Geochimica et Cosmochimica Acta, 64, 397–408.

Rosman K. and Taylor P. (1988)
Isotopic compositions of the elements 1997. Pure and Applied Chemistry, 70, 217–235.

Rosner M. and Meixner A. (2004)
Boron isotopic composition and concentration of ten geological reference materials. Geostandards and Geoanalytical Research, 28, 431–441.

Scambelluri M. and Tonarini S. (2012)
Boron isotope evidence for shallow fluid transfer across subduction zones by serpentinized mantle. Geology, 40, 907–910.

Tanaka R. and Nakamura E. (2005)
Boron isotopic constraints on the source of Hawaiian shield lavas. Geochimica et Cosmochimica Acta, 69, 3385–3399.

Thompson G., Bankston D.C. and Pasley S.M. (1970)
Trace element data for U.S.G.S. reference silicate rocks. Chemical Geology, 5, 215–221.

Tonarini S., Armienti P., D'Orazio M. and Innocenti F. (2001)
Subduction-like fluids in the genesis of Mt. Etna magmas: Evidence from boron isotopes and fluid mobile elements. Earth and Planetary Science Letters, 192, 471–483.

Tonarini S., Leeman W.P. and Leat P.T. (2011)
Subduction erosion of forearc mantle wedge implicated in the genesis of the South Sandwich Island (SSI) arc: Evidence from boron isotope systematics. Earth and Planetary Science Letters, 301, 275–284.

Tonarini S., Pennisi M., Adorni-Braccesi A., Dini A., Ferrara G., Gonfiantini R., Wiedenbeck M. and Gröning M. (2003)
Intercomparison of boron isotope and concentration measurements. Part I: Selection, preparation and homogeneity tests of the intercomparison materials. Geostandards Newsletter: The Journal of Geostandards and Geoanalysis, 27, 21–39.

Tonarini S., Pennisi M. and Leeman W.P. (1997)
Precise boron isotopic analysis of complex silicate (rock) samples using alkali carbonate fusion and ion-exchange separation. Chemical Geology, 142, 129–137.

Vils F., Tonarini S., Kalt A. and Seitz H.-M. (2009)
Boron, lithium and strontium isotopes as tracers of seawater–serpentinite interaction at Mid-Atlantic ridge, ODP Leg 209. Earth and Planetary Science Letters, 286, 414–425.

Walsh J.N. (1985)
Determination of boron at trace levels in rocks by inductively coupled plasma spectrometry. Analyst, 110, 959–962.

references

Wei G., Wei J., Liu Y., Ke T., Ren Z., Ma J. and Xu Y. (2013)
Measurement on high-precision boron isotope of silicate materials by a single column purification method and MC-ICP-MS. Journal of Analytical Atomic Spectrometry, 28, 606–612.

Xiao J., Xiao Y.K., Jin Z.D., He M.Y. and Liu C.Q. (2013)
Boron isotope variations and its geochemical application in nature. Australian Journal of Earth Sciences, 60, 431–447.

Xiao Y., Hoefs J., Simon K., Hou Z. and Zhang Z. (2011)
Fluid/rock interaction and mass transfer in continental subduction zones: Constraints from trace elements and isotopes (Li, B, O, Sr, Nd, Pb) in UHP rocks from the Chinese Continental Scientific Drilling Program, Sulu, East China. Contributions to Mineralogy and Petrology, 162, 797–819.

Yamaoka K., Ishikawa T., Matsubaya O., Ishiyama D., Nagaishi K., Hiroyasu Y., Chiba H. and Kawahata H. (2012)
Boron and oxygen isotope systematics for a complete section of oceanic crustal rocks in the Oman ophiolite. Geochimica et Cosmochimica Acta, 84, 543–559.

Yamaoka K., Matsukura S., Ishikawa T. and Kawahata H. (2015)
Boron isotope systematics of a fossil hydrothermal system from the Troodos ophiolite, Cyprus: Water–rock interactions in the oceanic crust and subseafloor ore deposits. Chemical Geology, 396, 61–73.

Yu J.M., Foster G.L., Elderfield H., Broecker W.S. and Clark E. (2010)
An evaluation of benthic foraminiferal B/Ca and $\delta^{11}B$ for deep ocean carbonate ion and pH reconstructions. Earth and Planetary Science Letters, 293, 114–120.

Zamboni D., Gazel E., Ryan J.G., Cannatelli C., Lucchi F., Atlas Z.D., Trela J., Mazza S.E. and De Vivo B. (2016)
Contrasting sediment melt and fluid signatures for magma components in the Aeolian Arc: Implications for numerical modeling of subduction systems. Geochemistry Geophysics Geosystems, 17, 2034–2053.

Zhang M., Zhang D., Zhao B., Wu M., Bao B., Liu Y. and Huang C. (2019)
Petrography and geochemistry of tourmaline breccia in the Longtoushan Au deposit, South China: Genesis and its exploration significance. Geochemistry: Exploration, Environment, Analysis, 19, 448–464.

Appendix A

Boron mass fraction and isotopic data from the literature for a selected range of geological reference materials. 'Mean' values correspond to means of all data from the literature and are reported in columns 'Literature' from Table 2. Literature data marked with an asterisk (*) have not been taken into account for the calculations of means, with results from this work reported in columns 'Combined' from Table 2.

Material	B mass fraction data ± 1*s*	Source	$\delta^{11}B_{SRM\ 951}$ data ± 1*s*	Source
	μg g^{-1}		‰	
B5	11.9 ± 0.2	Gonfiantini *et al.* (2003)	–	–
B5	10.3 ± 0.5	Gonfiantini *et al.* (2003)	–	–
B5	10.1 ± 0.5	Gonfiantini *et al.* (2003)	-3.71 ± 0.37	Romer *et al.* (2014)
B5	9.75 ± 0.04	Gonfiantini *et al.* (2003)	-3.86 ± 0.32	Pi *et al.* (2014)
B5	8.36 ± 0.12	Gonfiantini *et al.* (2003)	-3.50 ± 0.80	Pi *et al.* (2016)
B5	11.5 ± 0.4	Gonfiantini *et al.* (2003)	-4.30 ± 0.10	Hansen *et al.* (2017)
B5	10.0 ± 0.1	Gonfiantini *et al.* (2003)	-4.30 ± –	Berryman *et al.* (2017)
B5	10.1 ± 1.2	Gonfiantini *et al.* (2003)	-4.10 ± 2.70	Gonfiantini *et al.* (2003)
B5	8.42 ± 0.15	Tonarini *et al.* (2003)	-3.95 ± 0.32	Tonarini *et al.* (2003)
B5	8.48 ± 0.17	Tonarini *et al.* (2003)	-3.84 ± 0.32	Tonarini *et al.* (2003)
B5	9.27 ± 0.14	Pi *et al.* (2014)	-4.39 ± 0.53	Xiao *et al.* (2011)
B5	9.16 ± 0.13	Pi *et al.* (2016)	-3.60 ± 0.35	Wei *et al.* (2013)
B5	9.30 ± –	Berryman *et al.* (2017)	-4.69 ± 0.30	Li *et al.* (2019b)
Mean B5	***9.74 ± 1.10 (n = 13)***		***-4.02 ± 0.37 (n = 11)***	
JB-2	–	–	+6.96 ± 0.11	Pi *et al.* (2014)
JB-2	–	–	+7.66 ± 0.08	Leeman and Tonarini (2001)
JB-2	–	–	+5.79 ± 0.21 *	Leeman *et al.* (2004)
JB-2	–	–	+6.85 ± 0.12	Deyhle (2001)
JB-2	–	–	+7.66 ± 0.08	Dyar *et al.* (2001)
JB-2	–	–	+7.38 ± 0.21	Le Roux *et al.* (2004)
JB-2	–	–	+7.50 ± 0.22	Vils *et al.* (2009)
JB-2	30.0 ± 0.3	Jochum *et al.* (2016)	+7.14 ± 0.77	Kasemann *et al.* (2001)
JB-2	30.0 ± –	Govindaraju (1994)	+7.12 ± 0.34	Kasemann *et al.* (2001)
JB-2	30.4 ± 1.6	Kasemann *et al.* (2001)	+7.13 ± 0.10	Tonarini *et al.* (2001)
JB-2	29.6 ± 1.7	Leeman *et al.* (2017)	+7.33 ± 0.18	Tonarini *et al.* (2003)
JB-2	28.5 ± 1.8	Leeman *et al.* (2017)	+7.38 ± 0.11	Le Roux *et al.* (2004)
JB-2	30.2 ± –	Imai *et al.* (1995)	+7.25 ± 0.44	Le Roux *et al.* (2004)
JB-2	29.9 ± 1.5	Ishikawa *et al.* (2001)	+7.35 ± 0.44	Le Roux *et al.* (2004)
JB-2	28.4 ± 0.6	D'Orazio (1999)	+7.01 ± 0.05	Boschi *et al.* (2008)
JB-2	28.8 ± 0.7	Michel *et al.* (2015)	+7.95 ± 0.24	Chetelat *et al.* 2009
JB-2	31.2 ± 0.3	Lu *et al.* (2007)	+6.81 ± 0.11	Yamaoka *et al.* (2012)
JB-2	31.7 ± –	Gméling *et al.* (2005)	+6.83 ± 0.26	Lemarchand *et al.* (2012)
JB-2	30.8 ± –	Gméling *et al.* (2005)	+7.20 ± 0.26	Wei *et al.* (2013)
JB-2	30.4 ± 2.4	Dreyer *et al.* (2010)	+7.13 ± 0.10	Boschi *et al.* (2013)
JB-2	29.6 ± 0.2	Le Fevre and Ottolini (2006)	+7.30 ± 0.30	Genske *et al.* (2014)
JB-2	30.8 ± 0.1	Le Fevre and Ottolini (2006)	+7.25 ± 0.32	Harvey *et al.* (2014)
JB-2	29.7 ± 0.5	Mori *et al.* (2007)	+7.16 ± 0.31	Li *et al.* (2016)
JB-2	28.8 ± 0.9	Raffone *et al.* (2008)	+7.90 ± 1.03	Kimura *et al.* (2016)
JB-2	30.0 ± 1.0	Li *et al.* (2016)	+7.13 ± 0.10	Leeman *et al.* (2017)
JB-2	30.9 ± 0.5	Pi *et al.* (2014)	+7.38 ± 0.33	Li *et al.* (2019b)
Mean JB-2	***30.0 ± 0.9 (n = 19)***		***+7.21 ± 0.41 (n = 26)***	
JB-3	15.0 ± –	Govindaraju (1994)	–	–
JB-3	18.0 ± –	Imai *et al.* (1995)	–	–
JB-3	18.1 ± 0.8	D´Orazio (1999)	–	–
JB-3	20.3 ± 1.0	Ishikawa *et al.* (2001)	–	–
JB-3	20.0 ± 2.0	Rosner and Meixner (2004)	–	–
JB-3	20.9 ± –	Tanaka and Nakamura (2005)	–	–
JB-3	20.5 ± –	Tanaka and Nakamura (2005)	–	–
JB-3	21.5 ± –	Gméling *et al.* (2005)	–	–
JB-3	21.4 ± –	Gméling *et al.* (2005)	+5.89 ± 0.06	Pi *et al.* (2014)
JB-3	18.5 ± 0.7	Kurosawa *et al.* (2006)	+5.85 ± 0.41	Rosner and Meixner (2004)
JB-3	20.7 ± 0.2	Lu *et al.* (2007)	+6.50 ± –	Tanaka and Nakamura (2005)
JB-3	20.7 ± 0.1	Kitagawa *et al.* (2008)	+6.60 ± –	Tanaka and Nakamura (2005)

Appendix A (Continued).

Material	B mass fraction data ± 1*s*	Source	$\delta^{11}B_{SRM\ 951}$ data ± 1*s*	Source
	µg g^{-1}		‰	
JB-3	20.7 ± 0.6	Yamaoka *et al.* (2012)	+5.60 ± 0.10	Wei *et al.* (2013)
JB-3	19.4 ± 0.5	Li *et al.* (2016)	+5.83 ± 0.33	Li *et al.* (2016)
JB-3	16.4 ± 1.4	Zamboni *et al.* (2016)	+6.72 ± 0.07	Ishikawa *et al.* (2001)
JB-3	18.6 ± 1.8	Leeman *et al.* (2017)	+6.69 ± 0.12	Yamaoka *et al.* (2015)
JB-3	18.0 ± 0.8	Leeman *et al.* (2017)	+6.72 ± 0.07	Yamaoka *et al.* (2012)
JB-3	19.9 ± 0.2	Pi *et al.* (2014)	+6.78 ± –	Li *et al.* (2019b)
Mean JB-3	***19.4 ± 1.8 (n = 18)***		***+6.32 ± 0.46 (n = 10)***	
BCR-2	4.40 ± –	Jochum *et al.* (2016)	–	–
BCR-2	4.10 ± 0.60	Mori *et al.* (2007)	–	–
BCR-2	4.61 ± 0.01	Menard *et al.* (2013)	–	–
BCR-2	7.70 ± 1.80 *	Adam *et al.* (2014)	-5.90 ± 0.20	Wei *et al.* (2013)
BCR-2	4.00 ± 0.16	Peters *et al.* (2017)	-5.93 ± 0.27	Liu *et al.* (2018)
Mean BCR-2	***4.96 ± 1.55 (n = 5)***		***-5.92 ± 0.02 (n = 2)***	
BHVO-2	2.95 ± 0.83	Jochum *et al.* (2016)	–	–
BHVO-2	3.06 ± 0.06	Michel *et al.* (2015)	–	–
BHVO-2	3.12 ± –	Mohan *et al.* (2008)	–	–
BHVO-2	2.80 ± 0.30	Mori *et al.* (2007)	-0.70 ± 0.11	Wei *et al.* (2013)
BHVO-2	2.81 ± 0.05	Menard *et al.* (2013)	-1.61 ± 0.31	Liu *et al.* (2018)
Mean BHVO-2	***2.95 ± 0.14 (n = 5)***		***-1.16 ± 0.64 (n = 2)***	
JA-2	20.9 ± 2.1	Leeman *et al.* (2017)	–	–
JA-2	20.7 ± –	Imai *et al.* (1995)	–	–
JA-2	22.7 ± 0.3	Lu *et al.* (2007)	–	–
JA-2	19.4 ± 1.0	Kurosawa *et al.* (2006)	–	–
JA-2	20.5 ± 0.6	D'Orazio (1999)	–	–
JA-2	20.0 ± –	Mohan *et al.* (2008)	–	–
JA-2	21.4 ± –	Gméling *et al.* (2005)	–	–
JA-2	21.1 ± –	Gméling *et al.* (2005)	–	–
JA-2	19.9 ± 0.6	Leeman *et al.* (2017)	–	–
JA-2	21.1 ± 6.1	Jochum *et al.* (2016)	–	–
Mean JA-2	***20.8 ± 0.9 (n = 10)***		***-9.30 ± 0.45***	Wei *et al.* (2013)
AGV-1	7.80 ± –	Govindaraju (1994)	–	–
AGV-1	7.80 ± –	Smith (1995)	–	–
AGV-1	8.07 ± 0.12	Lu *et al.* (2007)	–	–
AGV-1	8.07 ± 0.56	Hu and Gao (2008)	–	–
AGV-1	8.10 ± –	Jochum *et al.* (2016)	–	–
Mean AGV-1	***7.97 ± 0.15 (n = 5)***		–	–
JR-2	135 ± –	Govindaraju (1994)	–	–
JR-2	158 ± 7	Kasemann *et al.* (2001)	–	–
JR-2	159 ± 6	Rosner *et al.* (2004)	+2.93 ± 0.12	Rosner and Meixner (2004)
JR-2	145 ± –	Imai *et al.* (1995)	+2.91 ± 0.48	Kasemann *et al.* (2001)
JR-2	174 *	Kasemann *et al.* (2001)	+2.51 ± 1.30	Kasemann *et al.* (2001)
JR-2	128 ± 9	Kurosawa *et al.* (2006)	+2.57 ± 0.53	Kasemann *et al.* (2001)
JR-2	168 ± –	Gméling *et al.* (2005)	+2.70 ± 0.28	Wei *et al.* (2013)
JR-2	168 ± –	Gméling *et al.* (2005)	+3.01 ± 0.51	Li *et al.* (2019b)
Mean JR-2	***154 ± 17 (n = 8)***		***+2.77 ± 0.21 (n = 6)***	
B6	205 ± 5	Gonfiantini *et al.* (2003)	–	–
B6	209 ± 2	Gonfiantini *et al.* (2003)	–	–
B6	197 ± 4	Gonfiantini *et al.* (2003)	–	–
B6	197 ± 1	Gonfiantini *et al.* (2003)	-3.20 ± 0.70	Gurenko *et al.* (2005)
B6	194 ± 10	Gonfiantini *et al.* (2003)	-3.30 ± 1.80	Gonfiantini *et al.* (2003)
B6	204 ± 6	Gonfiantini *et al.* (2003)	-1.61 ± 0.44	Tonarini *et al.* (2003)
B6	244 ± 5 *	Gonfiantini *et al.* (2003)	-1.68 ± 0.66	Tonarini *et al.* (2003)
B6	220 ± 1	Gonfiantini *et al.* (2003)	-1.60 ± 0.30	Wei *et al.* (2013)
B6	204 ± 9	Gonfiantini *et al.* (2003)	-2.59 ± 0.25	Devulder *et al.* (2015)
B6	206 ± 8	Tonarini *et al.* (2003)	-2.89 ± 0.80	Devulder *et al.* (2013)
B6	207 ± 10	Tonarini *et al.* (2003)	-3.29 ± 0.56	Hou *et al.* (2010)
B6	191 ± 4	Michel *et al.* (2015)	-2.76 ± 0.24	Li *et al.* (2019b)
Mean B6	***207 ± 14 (n = 12)***		***-2.55 ± 0.73 (n = 9)***	
JG-1	6.00 ± –	Govindaraju (1994)	–	–

Appendix A (Continued).

Material	B mass fraction data ± 1*s*	Source	$\delta^{11}B_{SRM\ 951}$ data ± 1*s*	Source
	µg g^{-1}		‰	
JG-1	6.87 ± –	Imai *et al.* (1995)	–	–
JG-1	6.03 ± 0.18	Michel *et al.* (2015)	–	–
Mean JG-1	***6.30 ± 0.49 (n = 3)***		–	–
JG-2	1.78 ± –	Imai *et al.* (1995)	–	–
JG-2	1.72 ± –	D'Orazio (1999)	–	–
JG-2	6.80 ± 0.90 *	Harvey *et al.* (1996)	–	–
JG-2	2.08 ± 0.03	Romer *et al.* (2014)	–	–
Mean JG-2	***3.10 ± 2.48 (n = 4)***		***-12.23 ± 0.40***	Romer *et al.* (2014)
SDC-1	12.8 ± –	Govindaraju (1994)	–	–
SDC-1	13.0 ± –	Smith *et al.* (1995)	–	–
Mean SDC-1	***12.9 ± 0.1 (n = 2)***		***-5.50 ± 0.35***	Wei *et al.* (2013)
B8	97.1 ± 1.2	Gonfiantini *et al.* (2003)	–	–
B8	95.7 ± 1.5	Gonfiantini *et al.* (2003)	–	–
B8	102 ± 1	Gonfiantini *et al.* (2003)	-4.75 ± 0.29	Romer *et al.* (2014)
B8	99.8 ± 1.7	Gonfiantini *et al.* (2003)	-5.47 ± 0.32	Pi *et al.* (2014)
B8	110 ± 3	Gonfiantini *et al.* (2003)	-5.30 ± –	Berryman *et al.* (2017)
B8	106 ± 1	Gonfiantini *et al.* (2003)	-5.60 ± 0.70	Gurenko *et al.* (2005)
B8	102 ± 5	Gonfiantini *et al.* (2003)	-5.40 ± 1.20	Gonfiantini *et al.* (2003)
B8	99.7 ± 1.5	Tonarini *et al.* (2003)	-4.75 ± 0.25	Tonarini *et al.* (2003)
B8	80.6 ± 2.9	Tonarini *et al.* (2003)	-4.60 ± 0.25	Tonarini *et al.* (2003)
B8	98.8 ± 1.7	Pi *et al.* (2014)	-4.90 ± 0.28	Pennisi *et al.* 2009
B8	94.0 ± –	Berryman *et al.* (2017)	-4.80 ± 0.22	Wei *et al.* (2013)
Mean B8	***98.7 ± 7.5 (n = 11)***		***-5.06 ± 0.38 (n = 9)***	
UB-N	140 ± 17	Govindaraju (1995)	–	–
UB-N	135 ± 1	Peters *et al.* (2017)	–	–
UB-N	157 ± –	D'Orazio (1999)	–	–
UB-N	140 ± –	Govindaraju (1994)	–	–
Mean UB-N	***143 ± 10 (n = 4)***		***+13.10 ± 0.21***	Wei *et al.* (2013)
PCC-1	1.40 ± –	Gladney *et al.* (1991)	–	–
PCC-1	1.40 ± 0.10	Gladney *et al.* (1991)	–	–
PCC-1	1.40 ± 0.20	Gladney *et al.* (1991)	–	–
PCC-1	2.00 ± –	Gladney *et al.* (1991)	–	–
PCC-1	2.20 ± 0.40	Gladney *et al.* (1991)	–	–
PCC-1	4.69 ± 0.33	Gladney *et al.* (1991)	–	–
PCC-1	6.00 ± –	Gladney *et al.* (1991)	–	–
PCC-1	12.8 ± –	Gladney *et al.* (1991)	–	–
Mean PCC-1	***3.99 ± 3.95 (n = 8)***		–	–

More than one representative value was chosen in some literature references because these values were obtained by different analytical methods.

$$\delta^{11}B_{SRM\,951} = \left({}^{11}B/{}^{10}B\right)_{sample} / \left({}^{11}B/{}^{10}B\right)_{SRM\,951} - 1$$